Remote mapping of foodscapes using sUAS and a low cost BG-NIR sensor

Laura ALONSO-MARTÍNEZ [1†], Miguel IBAÑEZ-ÁLVAREZ [2,†], Matthew BROLLY [3], Niall G. BURNSIDE [3], Juan A. CALLEJA[4,5,6], Marta PELÁEZ[7], Aida LÓPEZ-SÁNCHEZ[7], Jordi BARTOLOMÉ [2], Helena FANLO[1], Santiago LAVÍN[1], Ramón PEREA[7], Emmanuel SERRANO [1,8*]

1. Wildlife Ecology& Health group (WE&H), and Servei d'Ecopatologia de Fauna Salvatge (SEFaS). Departament de Medicina i Cirurgia Animals. Universitat Autònoma de Barcelona (UAB), Bellaterra, Spain
2. Grup de Recerca en Remugants. Departament de Ciència Animal i dels Aliments, Universitat Autònoma de Barcelona (UAB), Bellaterra, Spain
3. School of Environment & Technology, University of Brighton, Lewes Road, Brighton, BN2 4JG, UK
4. Universidad Autónoma de Madrid, Departamento de Biología (Botánica), Madrid, Spain
5. Centro de Investigación en Biodiversidad y Cambio Global, Madrid, Spain
6. CREAF, Cerdanyola del Vallès, Spain
7. Departamento de Sistemas y Recursos Naturales, Universidad Politécnica de Madrid, Madrid, Spain
8. Dipartimento di Scienze Veterinarie, Universitá di Torino, Grugliasco, Torino, Italy

† Equal contribution

*** Corresponding author**: emmanuel.serrano@uab.cat (ES)

Abstract

The assessment of landscape condition for large herbivores, also known as foodscapes, is fast gaining interest in conservation and landscape management programs worldwide. Although traditional approaches are now being replaced by satellite imagery, several technical issues still need to be addressed before full standardization of remote sensing methods for these purposes. We present a low-cost method, based on the use of a modified blue/green/near-infrared (BG-NIR) camera housed on a small-Unmanned Aircraft System (sUAS), to create foodscapes for a generalist Mediterranean ungulate: the Iberian Ibex (*Capra pyrenaica*) in Northeast Spain. Faecal cuticle micro-histological analyses were used to assess the dietary preferences of ibexes and then individuals of the most common plant species (n = 19) were georeferenced to use as test samples. Because of the seasonal pattern in vegetation activity, based on the NDVI (Smooth term $_{Month}$ = 21.5, p-value < 0.01, R^2 = 43%, from a GAM), images were recorded in winter and spring to represent contrasting vegetation phenology using two flight heights above ground level (30 and 60 m). Additionally, the range of image pixel sizes was 3.5-30 cm with the smallest pixel size representing the highest resolution. Boosted Trees were used to classify plant taxa based on spectral reflectance and create a foodscape of the study area. The number of target species, the sampling season, the height of flight and the image resolution were analysed to determine the accuracy of mapping the foodscape. The highest classification error (70.66%) was present when classifying all plant species using a 30cm pixel size from acquisitions at 30 m height. The lowest error (18.7%), however, was present when predicting plants preferred by ibexes, at 3.5 cm pixel size acquired at 60 m height. This methodology can help to successfully monitor food availability and seasonality and to identify individual species.

Key words: *Capra pyrenaica*, Food resources monitoring, Remote sensing, sUAS, Vegetation assessment

1. Introduction

The spatiotemporal assessment of food resources for large herbivores, also called foodscapes, is fast gaining interest within landscape and wildlife management, and associated research agendas worldwide. Knowing the distribution and availability of specific plants (i.e., used by ungulates see Espunyes et al., 2019), has become essential not only to understand population dynamics of herbivores but also those of their predators (Oates et al., 2019; Peters et al., 2019; Searle et al., 2007). Mapping vegetation is also essential for ecologists (Moore et al., 2010) and wildlife conservation agents (Schweiger et al., 2015a). Likewise, plant biodiversity conservation strongly depends on the interaction between plants and large herbivores, among others, (Boulanger et al., 2018; Royo et al., 2017). The modeling of these interactions is fast gaining interest (Weisberg and Coughenour, 2006), particularly by exploring plant communities at different spatial and temporal scales (Golodets et al., 2011; Schweiger et al., 2015a). Assessment of foodscapes is also of major concern for forest managers, as both wild and domestic ungulates influence forest regeneration, tree growth and forest development (Bergqvist et al., 2018; Rooney et al., 2015; Valle Júnior et al., 2019). Vegetation modulates both habitat and diet selection in large herbivores, which in turn affects the sign (mutualist vs. antagonist), the strength of plant-herbivore interactions (Gill, 1992; López-Sánchez et al., 2016; Perea et al., 2013) and their associated ecosystem services and disservices. In addition, ungulate species serve societal needs as game animals or subsistence foods (Carvalho et al., 2020), and can also affect agricultural crops which add importance to the understanding of nutritional resources and habitat use of large herbivores (Rowland et al., 2018; Duparc et al., 2019).

Traditionally, vegetation cover mapping has been done using field-based or *in situ* measurements (Karl et al., 2011). Although field studies are still required for calibration, and validation of other indirect approaches (e.g., based on remote sensing), they are time-consuming and often unfeasible when covering large areas. This is complicated further when studying complex landscapes across different seasons and years (Manousidis et al., 2016; Moore et al., 2010; Petersen et al., 2014; Royo et al., 2017). Remote sensing is thus becoming the main alternative to overcome the limitations of, and complement the advantages of field-based studies (Kerr and Ostrovsky, 2003; Pettorelli, 2013; Sankey et al., 2019; Skidmore et al., 2010). In fact, satellite derived-measurements are becoming popular for mapping vegetation cover, structure, composition, and condition in wide geographic areas and over long time periods (Harris et al., 2014, Wachendorf et al., 2017). However, several technical issues need to be addressed before remote sensing approaches can be fully established to create foodscapes. In homogeneous landscapes, for example, remote sensing methods are useful for mapping specific food resources e.g., lichens in tundra used by reindeer (see Falldorf et al., 2014), or linking the greenness of mixed-grass communities to diet quality of alpine ungulates (Schweiger et al., 2015b; Villamuelas et al., 2016). Few efforts, however, have been made to create foodscapes in complex, bushy and encroached landscapes such as those common in the Mediterranean region. To date, the most ambitious contributions in this area of science have achieved the assessment of the nutritional quality of specific tree species commonly used by African ungulates (Skidmore et al., 2010), and by Australian marsupials (Youngentob et al., 2012). Implementation and evaluation of the use of remote sensing to assess the availability of specific woody species used by ungulates in complex landscapes are still scarce but necessary.

One alternative, to gain definition in such heterogeneous environments, is the use of hyperspectral sensors set in unmanned aircraft systems (UAS, see Beeri et al., 2007; Schweiger et al., 2015b; Skidmore et al., 2010; Youngentob et al., 2012), or in combination with lidar (Insua et al., 2019; Lone et al., 2014; Pullanagari et al., 2018). Lamentably, these approaches are still expensive and remain outside of the budget capabilities of most organizations and companies, as well as government-funded bodies. Additionally, they show complexities that require additional expertise which inhibits the broader uptake and use by non-expert researchers and land managers alike. Thus, timely research in this field of remote sensing is required to support decision making, oriented towards the most appropriate, timely and low-cost methods available while also offering suitably high levels of accuracy (Wachendorf et al., 2017). Furthermore, although there are studies focused on estimating primary production and nutrient content, few of them integrate quality assessment and dietary species identification (food availability), and almost no studies focus simultaneously on heterogeneous environments and wide-ranging feeders.

Several methodological issues have to be solved to create foodscapes based on remote sensing. For example, when using UAS mounted sensors, it is important to define the altitude above ground level (AGL) to ensure coverage of the study area while also balancing against the pixel size and subsequent spatial resolution requirements of the study (Tommervik, 2014). Additionally, the spectral range and resolution requirements must be met by the sensor to ensure that detailed spectral responses for each pixel can be obtained. This is particularly relevant to accurately distinguish plant species and monitor their spectral responses and variations across different seasons (Hesketh and Sánchez-Azofeifa, 2012).

For these reasons, this study aims to address both challenges, heterogeneous environmental assessment and mixed feeder diet classification, using a simple and low cost 3 spectral band camera (modified to detect Blue, Green, and Near-Infrared (BG-NIR)) mounted on a small-Unmanned Aircraft System (sUAS). The study seeks to create a foodscape assessment for a mixed feeder ungulate, the Iberian Ibex (*Capra pyrenaica*), in a heterogeneous Mediterranean scrubland. Many sUAS are low-cost machines capable of carrying a wide range of sensors and imaging equipment to work in complex and heterogeneous scenarios (Anderson and Gaston, 2013), and similar sensors have successfully been employed in other vegetation studies (e.g., Gillan et al., 2019; Lu and He, 2017; Strong et al., 2017).

The Iberian Ibex is a mixed feeder with a diet including herbaceous and woody species (Alados and Escos, 1987; Martinez et al. 1985; Martinez and Martinez, 1987; R. García-González, 1992; Granados et al. 2001). This mountain ungulate shows great dietary plasticity but is influenced by plant phenology (Martinez, 2014; Martínez, 1994) and landscape characteristics (Martínez and Martínez, 1987; Moço et al., 2014; Perea et al., 2015).

In this paper, the primary aim is to determine the feasibility of remotely classifying Mediterranean plant species, in two periods of contrasting phenology, growing in a high diversity and physiognomically heterogeneous plant community, with special focus on the plants grazed or browsed by the Iberian Ibex diet. We do so by using a novel methodology and low budget equipment and seek to set a basis for further remote studies aimed at diet quality in complex environments.

2. Materials and methods

2.1. Study area

The study was undertaken in the National Game Reserve ‘‘Ports de Tortosa i Beseit’’ (NGRPTB) in Catalonia, northeast Spain (40º46’08’’ N, 0º20’04’’ E, 450 m. a.s.l., Figure 1). The average temperature in winter is from 0.4ºC to10ºC and in summer from 11ºC to 25ºC. Precipitation is concentrated in spring and autumn, with a mean rainfall of 133.7mm and 116.6 mm respectively. Summer is characterized by drought conditions, with an average precipitation of 29.97mm (Meteocat, 2019).

The study area is characterized by a Mediterranean sclerophyllous woody landscape, dominated by *Quercus ilex* and a dense scrubland integrated by more than 30 woody plants codominated by *Pistacia lentiscus*, *Erica multiflora, Quercus coccifera*, *Rosmarinus officinalis*, *Genista scorpius,* and *Ulex parviflorus*. Natural and planted Pine stands and isolated individuals (*Pinus nigra* and *Pinus pinaster*) were also present across the study area. More specifically, the investigation was conducted in a fenced scientific enclosure of 17 ha (see Figure 1), which maintained an introduced herd of 18 Iberian Ibexes. The enclosure facilitated the control of Ibex population numbers and represented all relevant vegetation communities and plant species typical of this Mediterranean landscape.

2.2. Field data collection

Field data were collected in both June 2018 and March 2019. The June period was selected to evaluate plants with new and well developed shoots and leaves, and the March period represented an inactive period (late winter) with plants harboring old shoots and leaves. It is hypothesised that spectral variations will be apparent across

all species on the two dates. In particular, higher NDVI values are expected to be higher in winter than in spring because of the higher photosynthetically active radiation of evergreen Mediterranean plants (Garbulsky et al., 2013).

Inside the enclosure, 11 plots of 15 x 15m were randomly distributed to obtain a representative vegetation sample from within the enclosure. A total of 19 representative plant species (from 12 family groups) were identified and sampled in the study site within the enclosure; and the height, shape, diameter of the vegetative crown and phenological stage were recorded and specifically sampled (for subsequent discernment in aerial imagery, Figure 2). The location of sampled individuals was recorded using a differential-GPS (Leica GS07) for image matching and all species coded for analysis (see Table 1). The number of individuals sampled ranged between 6 and 20 dependent upon species and vegetation state (see Table 1 and Figure 2). In addition, plant fragments were collected for further cuticle micro-histological analysis with up to 10 plants of each diet species sampled.

Finally, 10 fresh Ibex faecal samples were collected from around the enclosure. Fresh faecal samples were placed in individual plastic bags, labelled and then transported via a cool-box to the laboratory. Once at the laboratory, samples were stored in a freezer, at -20°C, until further processing.

2.3. Image acquisition and processing

A DJI Inspire 1 sUAS (DJI, Europe) was used to capture high-resolution aerial imagery of the study area. The sUAS captured imagery in consistent weather conditions (temperature *circa* 25^{o}C, wind speed < 7ms^{-1}, clear skies), and flights were conducted

198 at solar noon. On two consecutive days in June 2018, two separate flights were
199 undertaken; with a target altitude of 30 m AGL followed by 60 m AGL. On 25th of March
200 2019, one flight was undertaken with a target altitude of 30m. All flights followed a
201 cross-hatched flight plan to ensure maximum overlap (> 80%), at a 5m line spacing. A
202 low-cost payload sensor was used to collect imagery. More specifically, the payload
203 sensor was a BG-NIR modified version of the DJI X3 RGB sensor (12 megapixels,
204 DJI, Europe). The modified sensor was adjusted using a custom filter to pass infrared
205 light from the “red edge” at 680-800 nm, where plants actively reflect wavelengths,
206 and to block wavelengths over 800 nm. The filter ensured that the blue and green
207 channels only received visible light whilst allowing the detection of NIR light at 680-
208 800 nm (LDP LLC, Carlstadt, NJ, USA).

209 In addition, a total of 34 Ground Control Points (GCP) were located within the study
210 site to georeference the image in the later processing phase. A Leica GS07 dGPS was
211 used to record their coordinates. The sUAS was flown manually, and image capture
212 ranged between 83-162 images for 60 m AGL flights, and 450-563 images for 30 m
213 AGL flights in June, and between 190-1068 images in March (see table 2). All images
214 were recorded in JPEG file format and georeferenced to EXIF GPS coordinates and
215 altitude levels obtained from the DJI Inspire 1 sUAS.

216 The Pix4D Mapper® software was used to process all images. Initially, Structure-from-
217 Motion (SfM) was used to generate a Digital Surface Model of the study site (Westoby
218 et al., 2012), and then an orthomosaic generated by orthorectification of the aerial
219 imagery (Pix4D, 2018). This method removes perspective distortions from the images
220 using the Digital Surface Model.

To ensure consistency across all orthomosaics, the image resolution and pixel size were matched to the coarsest resolution across all final images using ArcGIS (v10.5.1). A nearest neighbour sampling method was used to resample discrete pixel data to larger pixel sizes, in order to test the possible influence on the image classification. The range of image pixel sizes was 3.5-30 cm, with the smallest pixel size representing the highest resolution consistently achievable during the sUAS flights.

Finally, using dGPS locations of the plants sampled in the field, a buffer was generated (25% of the smallest measured diameter of each specific plant) and used to extract the pixel values relative to each plant individually sampled. Pixel sampling of each plant was conducted in this way to avoid plant edges and soil reflectance where possible which may have caused disruptive pixel mixing. The resultant data provided BG-NIR pixel data for each plant sampled in the field which was used to perform subsequent analysis.

2.5. NDVI mapping

NDVI is a good indicator to reflect plant growth, quality, and phenology in Mediterranean ecosystems (Ogaya et al., 2015). NDVI represents the Normalised Difference Vegetation Index which is determined by calculating the difference in reflectance between the NIR band and a chosen visible band which is then divided by the sum of these two bands (Pettorelli, 2013). This index can be calculated for any individual pixel and typically uses the red band as the visible component due to the high level of absorption of this band during photosynthesis. The NIR band is used as it is highly reflected by healthy plants, allowing a strong contrast with the red visible

band. The blue band can be similarly used to the red band but is typically restricted to low altitude data acquisitions due to the negative effect of Rayleigh scattering that can interfere with satellite measurements as light passes through the atmosphere. It is more commonly referred to as Blue-NDVI (BNDVI) and has been used successfully in other vegetation assessment studies (Beeri et al., 2007; Lu and He, 2017). NDVI sensitivity to phenological stages of the plants was assessed as they manifested relevant seasonal phenological changes. Initially, satellite data were obtained to determine the mean NDVI values correspondent to the 2014-18 period for the entire study area, and to establish seasonal trends (MOD13Q1 NDVI data extracted from the MODIS repository, Moderate Resolution Imaging Spectroradiometer, provided by NASA). Secondly, the Blue-NDVI was calculated from the acquired images for all the plants recorded within the study area. The highest resolution images were used for these comparisons: June low flight 3.5cm pixel and March low flight 3.5 cm pixel. Single-band raster images were analysed and vegetation indices calculated from the sUAS captured imagery. These data were used to identify differences in vegetation index values and pixel values across sampled species and previously determined family groups.

2.6. Diet composition

Faecal cuticle micro-histological analysis was used to confirm that previous studies completed on the Iberian Ibex diet are suitable for this study area. A micro-histological analysis was therefore performed on the field sampled data. This technique facilitated the identification of plant epidermal fragments in the 10 samples collected in December 2019. Samples were prepared following treatment described by Bartolome

et al. (1995), with minor modifications. Approximately 10 g from the milled sample were placed in test tubes with 5 ml of 65% concentrated HNO_3. The test tubes were then boiled in a water bath at 80º C for 2 min. After digestion in HNO_3, the samples were diluted with 200 ml of water. This suspension was then passed through 1.00 mm and 0.125 mm filters. The 0.125-1.00 mm fraction was spread on glass microscope slides in a 50% aqueous glycerine solution and cover-slips were fixed with DPX micro-histological varnish. Three slides were prepared from each sample. The slides were examined under a microscope at 100-400x magnifications, conducting lengthwise traverses. Plant fragments were recorded and counted until 200 fragments of leaf epidermis were identified from each sample.

2.7. Classification analysis and Statistics

A machine learning algorithm approach was used to classify and map plant species across the study site. Machine learning algorithms are effective at operating on large volume and multivariate datasets. They can have high accuracy, and they have been successfully used when regression models are not suitable (Li et al., 2019; Marrs and Ni-Meister, 2019; Van Ewijk et al., 2014). In particular, the Breiman's Random Forests Model (RFM, Breiman, 2001) has been shown to be effective in other species distribution studies (see Carvalho et al., 2018; Zhang et al., 2019). Digital values of the three recorded bands (Blue, Green, NIR) were used as predictor variables. The effect of pixel size (3.5-30 cm), flight height, the month of sampling, and the response variable (e.g., all species vs diet species only) was assessed.

Initially, all the plant species sampled in the area were included in the RFM classification. Seventy percent of the sampled individuals were used as training data,

whilst the remaining 30% of sampled individuals were used as test data. The inclusion of the training data subset allowed independent assessment of the error in the classification method, using Out Of Bag (OOB) and Prediction Test Error (PTE). A confusion matrix was created, and the predictions evaluated against the independent ground-truthing data. The final error matrix was then used to select the most suitable image acquisition approach and processing method.

Following the assessment of all plant species, a further analysis was conducted to discriminate between those sampled species recognised as Ibex diet species according to our micro-histological results. This step was conducted in two ways. Initially, species were grouped according to diet and a secondary “other” species group was included; and secondly, only species recognised as Ibex diet species were included within the model, and the “other” species group was omitted from the analysis. As a further investigation, and to understand the source of the error and the relevance of potential methodological issues, a linear model was generated that predicted the percentage of error according to the pool of species included in the classification and the study season when images were captured.

Finally, a Principal Components Analysis (PCA) was undertaken to further explore the relationship between individual species, species pools and the three bands recorded by the sensor (BG-NIR). In addition, PCA score values were assessed across dietary species and used to discern differences in mean scores through an ANOVA post-hoc analysis.

2.8. Foodscape mapping

To complete the study a foodscape of the distribution of the main Iberian ibex resources in the study area was created. The original digital values of the already georeferenced pixels making up the orthomosaic were replaced by the predicted categories based on the RFM with the lowest test error. The procedure was done using the “rasterFromXYZ” function of the ”Raster” package, version 3.07 (Hijmans, 2019).

3. Results

3.1. NDVI

The traditional red band NDVI obtained from MODIS for the study area for the 2014-2018 period presents a clear seasonal pattern. In fact, 43% of the observed NDVI variability was explained by the effect of months (Smooth term $_{Month}$ = 21.5, p-value < 0.01, R^2 = 43%, from a GAM). A peak in primary production was shown in late winter (March) and a minimum in summer (June, Fig. 3A). March and June presented statistically significant differences between their NDVI values. The spatial resolution of the MODIS analysis provided a preliminary indicator of general NDVI trends in response to phenology which was then examined more specifically using the finer spatial resolution BG_NIR sensor.

In the absence of the red band, the BNDVI was used for the aerial data collection via the sUAS when analysing the NDVI values obtained for each recorded plant. Similar trends were obtained, across the two months studied using the sUAS mounted sensor, as found in the MODIS data. The differences between the values in both recorded months are shown in Fig. 3. Almost all species, 16 out of the 19 studied, have statistically significant differences in NDVI value between June and March (t-student

339 test with p-value < 0.05), except *Brachypodium retusum* (BR, p-value=0.1658),
340 *Helianthemum marifolium* (H, p-value=0.9869) and *Pinus pinaster* (PP, p-
341 value=0.1182).

342

343 3.2. Faecal cuticle micro-histological analysis

344 Faecal cuticle micro-histological analyses clearly show that diet composition of Ibexes
345 within the enclosure agrees with that in the base work (Martínez, 1994). Diet of Ibexes
346 was mainly based on non-legume wood species (ONLW), *Erica multifora* (EM),
347 graminoids (G, such as *Brachypodium phoenicoides* and *B. retusum*), Labiatae-
348 Asteraceae plants (L-A, e.g., *Rosmarinus officinalis*), and Fagaceae (e.g., *Quercus*
349 *ilex*). No plant represented more than 14% of use (Fig. 4), indicating the generalist
350 feeding behaviour of the species (Granados et al., 2001). As a result, species were
351 classified into five broad family groups with the species consistent in the diet across
352 all the year. The five groups were: *Quercus* spp. as the family Fagaceae (Group F*),*
353 *Rosmarinus officinalis* and *Thymus vulgaris* as the family Labiatae (Group L), *Erica*
354 *multiflora* (Group E), *Cistus albidus* (Group C), *Brachypodium phoenicoides, B.*
355 *retusum,* and other grass-like plants as Graminoids (Group G). The remaining species
356 were then placed into the category ‘Others’ that where excluded from the statistical
357 analysis.

358

359 3.3. Image capture and processing

The results showed that the orthomosaic images were created and georeferenced with an error of between 3 cm and 28 cm (see table 2), and the resultant single-band raster images used to calculate vegetation indices.

3.4. Random Forest Modelling.

The RFM was applied to all sUAS imagery collected in both June 2018 and March 2019 and assessed for classification error. The results from the RFM model indicate a consistent improvement in model performance using small pixel size (e.g., error reduction of 42.02% in predictions based on June flights at 60 m height and 3.5 cm pixel size see Table 3). In all RFM groups, the pixel size of 3.5 cm outperformed all other pixel size models. Moreover, it was found that as pixel size increased (up to 30 cm) model performance progressively deteriorated (Table 3).

Conversely, when flight height (60 m and 30 m) was compared (for similar pixel resolution), the RF model performance increased when the sUAS imagery was captured at a higher flight height. Although, comparatively speaking, the effect of this was not as substantial as the effect of pixel size on model performance (60 m flight vs 30 m flight; 3.5 cm pixel size; 6.6% increase in OOB error).

Further differences in model performance were observed when comparisons were made between survey season (June vs March). The model performance was better in June 2018 than in March 2019. The June 60 m flight outperformed the March 60 m flight, with a 9.5% reduction in OOB error rates (see Table 3).

Finally, the best performance by the RF model was observed when the response variable was changed to focus on specific Ibex diet species. Simplification of the

analysis to include only a ‘diet species’ group showed that the RF model’s OOB error rate dropped to only 18.4%; meaning a correct prediction of plants in 81.6% of instances. This pattern of error reduction was apparent in all flights using the diet response variables.

The above analysis is supported by the linear modelling undertaken. The analysis showed that both pools of species (e.g., all species and diet ones) and month (season) were significant variables. Interestingly, and in support once again, the species pool was shown to be the variable that most affects the error (p-value = 0.001, for the pool, and p-value = 0.03 for month). However, it is worth noting that the error calculated for the March 2019 surveys is higher in all pool scenarios than for June 2018 (Table 3, Fig. 1. Supplementary material).

3.5. Principal Component Analysis

Principal Component Analysis (PCA) was performed on the image data that provided the best classification results (June 2018, 30 m high flight, 3.5 cm pixel size). PCA was used to understand the behaviour of bands and vegetation indices, and to identify the different band responses for each species and their natural groupings. Evaluating the responses of the three recorded bands for all the recorded species provided the following results. The PCA axis 1 and 2 accounted for 97.9% of the variation in the dataset for the three spectral bands (Blue, Green, and Near Infrared). Axis 1 accounted for 82% of this variation with an associated elevated eigenvalue of 2.46. Axis 2 explained a further 15.9% (eigenvalue = 0.48) of the variation (Figure 2, supplementary material). In addition, the score values of each species were calculated (Figure 5) and demonstrated that axis 1 scores showed the greatest potential to

represent the variation of the spectral responses to the three bands. ANOVA test and corresponding post-hoc analyses showed statistically significant differences between the reflectance values of all plant species. However, it is worth noting that, this could be a false discovery rate due to effect size; as there were many sampled individuals (246) and therefore many pixels (up to 66264, in the data set of June 2018, 30 m flight height, and 3.5 cm pixel size, high flight, and June). To further understand the variability within species the above analysis was repeated accounting for solely the dietary species.

Evaluating the spectral response of each individual to the three recorded bands provided the following results. The PCA axis 1 and 2 accounted for the same proportion (97.9%) of the variation observed in the spectral responses across all individuals. Axis 1 accounted for 82% of the variation (eigenvalue = 2.50), and axis 2 explained a further 15% (eigenvalue = 0.44) of the variation (Figure 3, supplementary material). In addition, the score values of each plant group were calculated to illustrate the differences. Post-hoc analysis revealed significant differences between all dietary groups except for the pair *Labiatae* and *Erica multiflora* (p-value = 0.0628, Figure 6).

3.6. Foodscape mapping

The foodscape map on Fig. 7 predicts that 13.04% of the study area is covered by Fagaceae plants (Group F), 4.08% by graminoids (Group G), 2.23% by Labiateae (e.g., *Rosmarinus* and *Thymus*, Group L), 1.77% by *Erica multiflora* (Group E) and 0.02% by *Cistus albidus* (Group C). Most of the area (78.06%), however, included other plants not found in the Ibex diet, bare soil and rocks.

4. Discussion

This study has successfully explored the application of a modified BG-NIR sensor, mounted on a low cost sUAS, to create foodscapes for a mixed feeder in a Mediterranean scrubland, rich in woody species with very different physiognomies.

Analysis has shown successful discrimination of species within a species rich and physiognomically heterogeneous Mediterranean scrubland. Plant prediction was correct in 81.6% of instances (prediction error 18.4%) when using a training data set of 173 individuals (73 in the test dataset) representing all the most abundant species at the study site. Plant prediction improved further to 88.2% when focussing on the Ibex diet species alone (prediction error 11.8%) using a training data set of 97 individuals (and a test dataset of 41). Such errors are similar or, in some case, lower than those obtained by using hyperspectral methodologies in complex ecosystems (e.g., Clark et al., 2005; Ferreira et al., 2016), including Mediterranean ones (e.g., (Manevski et al., 2012).

Our classification results along with those of the PCA analysis, show a wide range of spectral responses across the species investigated, but also a useable level of homogeneity within species groups; when considering both ‘all species’ and only those ‘within the Ibex diet’. These results indicate that successful classification is possible. The success of using only 3 spectral bands to identify significantly different spectral responses across species and similarities within species groups, coupled with the high level accuracy of classification, outline the feasibility and potential for such a low-cost application to develop foodscapes and facilitate their long-term management.

453 The success in discriminating Ibex diet species remotely provides a strong foundation
454 from which to discuss the technical issues in the classification process. Initially, the
455 results indicate that small pixel size provides better classification results; as previously
456 reported in other studies (Hsieh et al., 2001; Hu et al., 2019) which discuss the
457 relevance of pixel size in classification performance and the effect of variations in plant
458 size and ground coverage. However, for the same pixel size, higher flights have shown
459 to perform better than lower flights, which is similar to other methodological studies
460 (e.g., Mesas-Carrascosa et al., 2015). The study by Mesas-Carrascosa et al. (2015)
461 indicated that there was greater discrimination between species at higher flights. In
462 addition, higher altitudes typically have less perspective distortion as the ratio of the
463 topographic change to flying altitude is smaller; hence, the accuracy of the orthophoto
464 can be higher; as is reflected in the work of Nesbit and Hugenholtz, (2019). Therefore,
465 when choosing the ideal flight parameters (as pixel size is determined by both sensor
466 type and flight height) a balance between both must be found; taking into account the
467 area to evaluate, the flight platform employed, and the financial and time costs.

468 This study has also shown that season is a relevant factor when working with plant
469 species in temperate regions since they manifest different physiological status and
470 even morphologies throughout the year (see also Sperlich et al., 2014., Vogt and
471 Gerhard Gul, 1994). Our results show that the most suitable season to perform the
472 classification study at this site is June (vs March) when most of the Mediterranean
473 woody taxa end their growth and flowering. Thus, plants have a large part of their
474 vegetative structure (not woody) renewed, with its characteristic morphology. At a
475 tissue and chemical level, the Mediterranean woody plants are fully constituted to be
476 able to withstand the water deficit and the severe heat stroke of the summer that starts
477 in June (Fernández-Marín et al., 2017). All these characteristics along with net inter-

species differences in water content (related to drought adaptations) determine the optical properties of the plants (Manevski et al., 2012). Due to its influence on the classification results the importance of prior knowledge of the phenological pattern of the area and the present plant species could be crucial to applying this methodology over a wider area and for it to not be restricted by site specific conditions.

In our study the classification results improved when focusing on the target diet species (Prediction error reduced to 11.8%). The result showed that the pool of training species influenced classification success with accuracy reported of 88.2%. This clearly indicates that an informed knowledge of the target diet species for the study area is of great value to maximise classification accuracy. Our results show that the classification accuracy can be improved by over 6%. Moreover, the importance of the micro-histological analysis or other related diet studies is evident in this process. However, caution is needed here given the associated reduction in both test and training data samples. The micro-histological analysis has served as an effective tool, focussing and reducing the pool of input species identified as diet species and subsequently improving the relevance and overall classification performance. Reducing the number of diet species classes by combining similar species, for example logically grouping *Pinus pinaster* and *P. nigra* as Pines, and *Brachypodium phoenicoides* and *B. restusum* as Graminoids offered further improvement in classification accuracy but was limited to an increase of 0.5-2%, with no significant improvement given the reduced specificity of the classification.

Regarding the obtained error, it is also relevant to consider the size (and biotype) of the plants. This seems to be case of *Helianthemum marifolium*, a representative taxon of typical prostrated chamaephytic communities on Mediterranean bedrocks. These small prostrated plants, with diameters around the calibration error (*circa* 20 cm) and

503 loose branching on bare soils, appeared to yield higher errors in classification
504 compared to those of bigger and thicker plants. These finding are similar to other
505 recent, and related, studies in rangeland ecosystems where small shrub/subshrub
506 species, with low abundance, were found to have reduced classification success
507 (Sankey et al., 2019).

508 However, with the relative successes of our study, when focussing on target diet
509 species, areas for improvement are largely focussed on the sensor rather than on the
510 methodology adopted. Improvements are most likely to be achieved by increasing the
511 sensitivity of spectral responses to plant species variation, and taking advantage of
512 the increased spectral resolution of more expensive cameras. Although the low-cost
513 aspect of this study is a unique selling point, upgrading to a more expensive
514 hyperspectral camera could offer greater flexibility, and potentially accuracy, during
515 the classification process (Manevski et al., 2012; Sankey et al., 2019). Known as
516 hyperspectral sensors these cameras can offer a greater quantity of spectral bands
517 but also bands of finer spectral resolution and have been used advantageously in
518 several other works (Beeri et al., 2007; Lone et al., 2014). However, with this
519 consideration, one of the relevant achievements of this work should not be
520 compromised. This being the creation of an accessible and affordable tool for land
521 managers and researchers to be applied in heterogeneous landscapes and on animals
522 with species-specific diet accounting for the general ecosystem characteristics
523 including plant species composition.

524

525 5. Conclusion

This feasibility study outlines the possibility of describing food location for a mixed herbivore in a heterogeneous environment. A modified BG-NIR camera, mounted on a low cost sUAS, has been shown to be successful in classifying plant species and to describe the foodscapes of ungulates such as Ibex. The benefits of this study, the methodology presented, and the potential for further development are applicable to studies of wild and domestic herbivore distribution and welfare, predator distribution, vegetation changes, and habitat biodiversity internationally (Boulanger et al., 2018; Moore et al., 2010; Oates et al., 2019; Peters et al., 2019; Searle et al., 2007)

Further studies with hyperspectral cameras are necessary to assess the improvements hypothesised, and the potential enhancement of efficiency and accuracy offered by an increased quantity and refined nature of spectral information. Additionally, it would be interesting to increase the number of sampling months in order to fully study plant availability throughout the year. Further research should be done in order to evaluate diet quality by improving and refining the affordable, accessible and non-time consuming methods that would be beneficial to land managers. Moreover, following the methodology describe here, we might be able to predict feeding behaviour across seasons and according to relevant meteorological events and landscape changes. To do this, we should also have more information about plants physiology and ibex diet data across seasons. The classification results obtained in this study provide a strong foundation on which to develop such diet quality studies.

Acknowledgments

We are grateful to the Department of Agriculture, Cattle, Fisheries and Food of the Catalonian Government, and the successive Heads and Technicians of the Ports de Tortosa I Beseit National Game Reserve, but in particular Xavier Olive, and Juanjo Estrada, for the support provided during the study period. This work has been funded by the Spanish Ministerio de Ciencia, Innovación y Universidades through the INCREMENTO project (RTI2018-094202-BC21). ES is supported by the Spanish Ministerio de Ciencia Innovación y Universidades (MICINN) through a Ramon y Cajal agreement (RYC-2016-21120).

References

Alados, C.L., Escos, J., 1987. Relationships between movement rate, agonistic displacements and forage availability in spanish ibexes (*Capra pyrenica*). Biol. Behav. 12, 245–255.

Anderson, K., Gaston, K.J., 2013. Lightweight unmanned aerial vehicles will revolutionize spatial ecology. Front. Ecol. Environ. 11, 138–146. https://doi.org/10.1890/120150

Bartolome, J., Franch, J., Gutman, M., Seligman, N.G., 1995. Physical Factors That Influence Fecal Analysis Estimates of Herbivore Diets. J. Range Manag. 48, 267. https://doi.org/10.2307/4002432

Beeri, O., Phillips, R., Hendrickson, J., Frank, A.B., Kronberg, S., 2007. Estimating forage quantity and quality using aerial hyperspectral imagery for northern mixed-grass prairie. Remote Sens. Environ. 110, 216–225. https://doi.org/10.1016/j.rse.2007.02.027

Bergqvist, G., Wallgren, M., Jernelid, H., Bergström, R., 2018. Forage availability and moose winter browsing in forest landscapes. For. Ecol. Manage. 419–420, 170–178. https://doi.org/10.1016/j.foreco.2018.03.049

Boulanger, V., Dupouey, J.L., Archaux, F., Badeau, V., Baltzinger, C., Chevalier, R., Corcket, E., Dumas, Y., Forgeard, F., Mårell, A., Montpied, P., Paillet, Y., Picard, J.F., Saïd, S., Ulrich, E., 2018. Ungulates increase forest plant species richness to the benefit of non-forest specialists. Glob. Chang. Biol. 24, e485–e495. https://doi.org/10.1111/gcb.13899

Breiman, L., 2001. ST4_Method_Random_Forest. Mach. Learn. 45, 5–32. https://doi.org/10.1017/CBO9781107415324.004

Carvalho, J., Büntgen, U.L.F., Pettorelli, N., Mentaberre, G., Boix, X.O., Eizaguirre, O., Pérez, J.M., Fandos, P., Torres, R.T., Lavín, S., Fonseca, C., Serrano, E., 2020. Habitat and Harvesting Practices In fl uence Horn Growth of Male Ibex. J. Wildl. Manage. https://doi.org/10.1002/jwmg.21830

Carvalho, J., Santos, J.P.V., Torres, R.T., Santarém, F., Fonseca, C., 2018. Tree-based methods: Concepts, uses and limitations under the framework of resource selection models. J. Environ. Informatics 32, 112–124. https://doi.org/10.3808/jei.201600352

Clark, M.L., Roberts, D.A., Clark, D.B., 2005. Hyperspectral discrimination of tropical rain forest tree species at leaf to crown scales. Remote Sens. Environ. 96, 375–398. https://doi.org/10.1016/j.rse.2005.03.009

Duparc, A., Garel, M., Marchand, P., Dubray, D., Maillard, D., Loison, A., 2019. Through the taste buds of a large herbivore: foodscape modeling contributes to an understanding of forage selection processes. Oikos. https://doi.org/10.1111/oik.06386

Espunyes, J., Bartolomé, J., Garel, M., Gálvez-Cerón, A., Aguilar, X.F., Colom-Cadena, A., Calleja, J.A., Gassó, D., Jarque, L., Lavín, S., Marco, I., Serrano, E., 2019. Seasonal diet composition of Pyrenean chamois is mainly shaped by primary production waves. PLoS One 14, 1–23. https://doi.org/10.1371/journal.pone.0210819

Falldorf, T., Strand, O., Panzacchi, M., Tømmervik, H., 2014. Estimating lichen volume and reindeer winter pasture quality from Landsat imagery. Remote Sens. Environ. 140, 573–579. https://doi.org/10.1016/j.rse.2013.09.027

Fernández-Marín, B., Hernández, A., Garcia-Plazaola, J.I., Esteban, R., Míguez, F., Artetxe, U., Gómez-Sagasti, M.T., 2017. Photoprotective strategies of mediterranean plants in relation to morphological traits and natural environmental pressure: A meta-analytical approach. Front. Plant Sci. 8. https://doi.org/10.3389/fpls.2017.01051

Ferreira, M.P., Zortea, M., Zanotta, D.C., Shimabukuro, Y.E., de Souza Filho, C.R., 2016. Mapping tree species in tropical seasonal semi-deciduous forests with hyperspectral and multispectral data. Remote Sens. Environ. 179, 66–78. https://doi.org/10.1016/j.rse.2016.03.021

Garbulsky, M.F., Peñuelas, J., Ogaya, R., Filella, I., 2013. Leaf and stand-level carbon uptake of a Mediterranean forest estimated using the satellite-derived reflectance indices EVI and PRI. Int. J. Remote Sens. 34, 1282–1296. https://doi.org/10.1080/01431161.2012.718457

Gill, R.M.A., 1992. A review of damage by mammals in north temperate forests: 3. Impact on trees and forests. Forestry 65, 363–388. https://doi.org/10.1093/forestry/65.4.363-a

Gillan, J.K., McClaran, M.P., Swetnam, T.L., Heilman, P., 2019. Estimating forage utilization with drone-based photogrammetric point clouds. Rangel. Ecol. Manag. 72, 575–585. https://doi.org/10.1016/j.rama.2019.02.009

Golodets, C., Kigel, J., Sternberg, M., 2011. Plant diversity partitioning in grazed Mediterranean grassland at multiple spatial and temporal scales. J. Appl. Ecol. 48, 1260–1268. https://doi.org/10.1111/j.1365-2664.2011.02031.x

Granados, J.E., Pérez, J.M., Márquez, F.J., Serrano, E., Soriguer, R.C., Fandos, P., 2001. LA CABRA MONTÉS (Capra. Galemys 13, 3–37.

Harris, A., Carr, A.S., Dash, J., 2014. Remote sensing of vegetation cover dynamics and resilience across southern Africa. Int. J. Appl. Earth Obs. Geoinf. 28, 131–139. https://doi.org/10.1016/j.jag.2013.11.014

Hesketh, M., Sánchez-azofeifa, G.A., 2012. Remote Sensing of Environment The effect of seasonal spectral variation on species classi fi cation in the Panamanian tropical forest. Remote Sens. Environ. 118, 73–82. https://doi.org/10.1016/j.rse.2011.11.005

Hijmans, R.J., 2019. Introduction to the 'raster' package (version 3.0-7) 1–250.

Hsieh, P.F., Lee, L.C., Chen, N.Y., 2001. Effect of spatial resolution on classification errors of pure and mixed pixels in remote sensing. IEEE Trans. Geosci. Remote Sens. 39, 2657–2663. https://doi.org/10.1109/36.975000

Hu, P., Guo, W., Chapman, S.C., Guo, Y., Zheng, B., 2019. Pixel size of aerial imagery constrains the applications of unmanned aerial vehicle in crop breeding. ISPRS J. Photogramm. Remote Sens. 154, 1–9. https://doi.org/10.1016/j.isprsjprs.2019.05.008

Insua, J.R., Utsumi, S.A., Basso, B., 2019. Estimation of spatial and temporal variability of pasture growth and digestibility in grazing rotations coupling unmanned aerial vehicle (UAV) with crop simulation models. PLoS One 14, 1–13. https://doi.org/10.1371/journal.pone.0212773

Karl, J.W., Colson, K., Swartz, H., 2011. Rangeland Assessment and Monitoring Methods Guide: An interactive tool for selecting methods for assessment and monitoring. Rangelands 33, 48–54. https://doi.org/10.2111/1551-501X-33.4.48

Kerr, J.T., Ostrovsky, M., 2003. From space to species: Ecological applications for remote sensing. Trends Ecol. Evol. 18, 299–305. https://doi.org/10.1016/S0169-5347(03)00071-5

Li, Z., Zan, Q., Yang, Q., Zhu, D., Chen, Y., Yu, S., 2019. Remote Estimation of Mangrove Aboveground Carbon Stock at the Species Level Using a Low-Cost Unmanned Aerial Vehicle System. Remote Sens. 11, 1018. https://doi.org/10.3390/rs11091018

Lone, K., Van Beest, F.M., Mysterud, A., Gobakken, T., Milner, J.M., Ruud, H.P., Loe, L.E., 2014. Improving broad scale forage mapping and habitat selection analyses with airborne laser scanning: The case of moose. Ecosphere 5, 1–22. https://doi.org/10.1890/ES14-00156.1

López-Sánchez, A., Perea, R., Dirzo, R., Roig, S., 2016. Livestock vs. wild ungulate management in the conservation of Mediterranean dehesas: Implications for oak regeneration. For. Ecol. Manage. 362, 99–106. https://doi.org/10.1016/j.foreco.2015.12.002

Lu, B., He, Y., 2017. Species classification using Unmanned Aerial Vehicle (UAV)-acquired high spatial resolution imagery in a heterogeneous grassland. ISPRS J. Photogramm. Remote Sens. 128, 73–85. https://doi.org/10.1016/j.isprsjprs.2017.03.011

Manevski, K., Manakos, I., Petropoulos, G.P., Kalaitzidis, C., 2012. Spectral discrimination of mediterranean maquis and phrygana vegetation: Results from a case study in Greece. IEEE J. Sel. Top. Appl. Earth Obs. Remote Sens. 5, 604–616. https://doi.org/10.1109/JSTARS.2012.2190044

Manousidis, T., Kyriazopoulos, A.P., Parissi, Z.M., Abraham, E.M., Korakis, G., Abas, Z., 2016. Grazing behavior , forage selection and diet composition of goats in a Mediterranean woody rangeland. Small Rumin. Res. https://doi.org/10.1016/j.smallrumres.2016.11.007

Marrs, J., Ni-Meister, W., 2019. Machine Learning Techniques for Tree Species Classification Using Co-Registered LiDAR and Hyperspectral Data. Remote Sens. 11, 819. https://doi.org/10.3390/rs11070819

Martinez, T., 2014. Diet selection by Spanish ibex in early summer in Sierra Nevada. Acta Theriol. (Warsz). 45, 335–346. https://doi.org/10.4098/at.arch.00-33

Martínez, T., 1994. Dieta estacional de la cabra montés (Capra pyrenaica) en los Puertos de Tortosa y Beceite (área Mediterranea del Nordeste de España). Ecología 8, 373–380.

Martinez, T., Martinez, E., 1987. in spring and summer at the Sierra de Credos , Spain.

Martinez, T., Martinez, E., Fandos, P., 1985. Composition of the food of the Spanish Wild Goat in Sierras de Cazorla and Segura, Spain. Acta Theriol. (Warsz). 30, 461–494. https://doi.org/10.4098/at.arch.85-31

Mesas-Carrascosa, F.J., Torres-Sánchez, J., Clavero-Rumbao, I., García-Ferrer, A., Peña, J.M., Borra-Serrano, I., López-Granados, F., 2015. Assessing optimal flight parameters for generating accurate multispectral orthomosaicks by uav to support site-specific crop management. Remote Sens. 7, 12793–12814. https://doi.org/10.3390/rs71012793

Meteocat, 2019. Anuari de dades meteorològiques - PN dels Ports, X5 (Baix Ebre). Serv. Meterològic Catalunya. http//www.meteo.cat/wpweb/climatologia/serveis-i-dades-climatiques/anuaris-de-dades-meteorologiques/xarxa-destacions-meteorologiques-automatiques/.

Moço, G., Serrano, E., Guerreiro, M., Ferreira, A.F., Petrucci-Fonseca, F., Santana, D., Maia, M.J., Soriguer, R.C., Pérez, J.M., 2014. Does livestock influence the diet of Iberian ibex Capra pyrenaica in the Peneda-Gerês National Park (Portugal)? Mammalia 78, 393–399. https://doi.org/10.1515/mammalia-2013-0139

Moore, B.D., Lawler, I.R., Wallis, I.R., Beale, C.M., Foley, W.J., 2010. Palatability mapping: A koala's eye view of spatial variation in habitat quality. Ecology 91, 3165–3176. https://doi.org/10.1890/09-1714.1

Nesbit, P.R., Hugenholtz, C.H., 2019. Enhancing UAV-SfM 3D model accuracy in high-relief landscapes by incorporating oblique images. Remote Sens. 11. https://doi.org/10.3390/rs11030239

Oates, B.A., Merkle, J.A., Kauffman, M.J., Dewey, S.R., Jimenez, M.D., Vartanian, J.M., Becker, S.A., Goheen, J.R., 2019. Antipredator response diminishes during periods of resource deficit for a large herbivore. Ecology 100, 1–8. https://doi.org/10.1002/ecy.2618

Ogaya, R., Barbeta, A., Başnou, C., Peñuelas, J., 2015. Satellite data as indicators of tree biomass growth and forest dieback in a Mediterranean holm oak forest. Ann. For. Sci. 72, 135–144. https://doi.org/10.1007/s13595-014-0408-y

Perea, R., Delibes, M., Polko, M., Suárez-Esteban, A., Fedriani, J.M., 2013. Context-dependent fruit-frugivore interactions: Partner identities and spatio-temporal variations. Oikos 122, 943–951. https://doi.org/10.1111/j.1600-0706.2012.20940.x

Perea, R., Perea-García-Calvo, R., Díaz-Ambrona, C.G., San Miguel, A., 2015. The reintroduction of a flagship ungulate Capra pyrenaica: Assessing sustainability by surveying woody vegetation. Biol. Conserv. 181, 9–17. https://doi.org/10.1016/j.biocon.2014.10.018

Peters, W., Hebblewhite, M., Mysterud, A., Eacker, D., Hewison, A.J.M., Linnell, J.D.C., Focardi, S., Urbano, F., De Groeve, J., Gehr, B., Heurich, M., Jarnemo, A., Kjellander, P., Kröschel, M., Morellet, N., Pedrotti, L., Reinecke, H., Sandfort, R., Sönnichsen, L., Sunde, P., Cagnacci, F., 2019. Large herbivore migration plasticity along environmental gradients in Europe: life-history traits modulate forage effects. Oikos 128, 416–429. https://doi.org/10.1111/oik.05588

Petersen, C.A., Villalba, J.J., Provenza, F.D., Petersen, C.A., Villalba, J.J., Provenza, F.D., 2014. Influence of Experience on Browsing Sagebrush by Cattle and Its Impacts on Plant Community Structure Influence of Experience on Browsing Sagebrush by Cattle and Its Impacts on Plant Community Structure 67, 78–87. https://doi.org/10.2111/REM-D-13-00038.1

Pettorelli, N., 2013. Satellite Data-Based Indices to Monitor Land Use and Habitat Changes, in: Biodiversity Monitoring and Conservation: Bridging the Gap between Global Commitment and Local Action. pp. 95–119. https://doi.org/10.1002/9781118490747.ch5

Pullanagari, R.R., Kereszturi, G., Yule, I., 2018. Integrating airborne hyperspectral, topographic, and soil data for estimating pasture quality using recursive feature elimination with random forest regression. Remote Sens. 10. https://doi.org/10.3390/rs10071117

R. García-González, P.C., 1992. 37_Feeding_Strat.Pdf.

Rooney, T., 2015. Integrating Ungulate Herbivory into Forest Landscape Restoriation.

Rowland, M.M., Wisdom, M.J., Nielson, R.M., Cook, J.G., Cook, R.C., Johnson, B.K., Coe, P.K., Hafer, J.M., Naylor, B.J., Vales, D.J., Anthony, R.G., Cole, E.K., Danilson, C.D., Davis, R.W., Geyer, F., Harris, S., Irwin, L.L., Mccoy, R., Pope, M.D., Sager-fradkin, K., Vavra, M., Hellgren, E.C., 2018. Modeling elk nutrition and habitat use in Western Oregon and Washington. Wildl. Monogr. 199, 1–69.

Royo, A.A., Kramer, D.W., Miller, K. V., Nibbelink, N.P., Stout, S.L., 2017. Spatio-temporal variation in foodscapes modifies deer browsing impact on vegetation. Landsc. Ecol. 32, 2281–2295. https://doi.org/10.1007/s10980-017-0568-x

Sankey, T.T., Leonard, J.M., Moore, M.M., 2019. Unmanned Aerial Vehicle − Based Rangeland Monitoring: Examining a Century of Vegetation Changes. Rangel. Ecol. Manag. 72, 858–863. https://doi.org/10.1016/j.rama.2019.04.002

Schweiger, A.K., Risch, A.C., Damm, A., Kneubühler, M., Haller, R., Schaepman, M.E., Schütz, M., 2015a. Using imaging spectroscopy to predict above-ground plant biomass in alpine grasslands grazed by large ungulates. J. Veg. Sci. 26, 175–190. https://doi.org/10.1111/jvs.12214

Schweiger, A.K., Schütz, M., Anderwald, P., Schaepman, M.E., Kneubühler, M., Haller, R., Risch, A.C., 2015b. Foraging ecology of three sympatric ungulate species - behavioural and resource maps indicate differences between chamois, ibex and red deer. Mov. Ecol. 3, 6. https://doi.org/10.1186/s40462-015-0033-x

Searle, K.R., Hobbs, N.T., Gordon, I.J., 2007. It's the "Foodscape", not the Landscape: Using Foraging Behavior to Make Functional Assessments of Landscape Condition. Isr. J. Ecol. Evol. 53, 297–316. https://doi.org/10.1560/ijee.53.3.297

Skidmore, A.K., Ferwerda, J.G., Mutanga, O., Van Wieren, S.E., Peel, M., Grant, R.C., Prins, H.H.T., Balcik, F.B., Venus, V., 2010. Forage quality of savannas - Simultaneously mapping foliar protein and polyphenols for trees and grass using hyperspectral imagery. Remote Sens. Environ. 114, 64–72. https://doi.org/10.1016/j.rse.2009.08.010

Sperlich, D., Chang, C.T., Peñuelas, J., Gracia, C., Sabaté, S., 2014. Foliar photochemical processes and carbon metabolism under favourable and adverse winter conditions in a Mediterranean mixed forest, Catalonia (Spain). Biogeosciences Discuss. 11, 9697–9759. https://doi.org/10.5194/bgd-11-9697-2014

Stout, S.L., Kramer, D.W., Miller, K. V, Nibbelink, N.P., 2018. Spatio-temporal variation in foodscapes modifies deer browsing impact on vegetation Spatio-temporal variation in foodscapes modifies deer browsing impact on vegetation. Landsc. Ecol. https://doi.org/10.1007/s10980-017-0568-x

Strong, C.J., Burnside, N.G., Llewellyn, D., 2017. The potential of small-Unmanned Aircraft Systems for the rapid detection of threatened unimproved grassland communities using an Enhanced Normalized Difference Vegetation Index. PLoS One 12, 1–16. https://doi.org/10.1371/journal.pone.0186193

Tommervik, H., 2014. Use of Unmanned Aircraft Systems (Uas) in a Multi-Scale Vegetation Index Study 75, 47–52. https://doi.org/10.12760/02-2014-1-09

Valle Júnior, R.F. do, Siqueira, H.E., Valera, C.A., Oliveira, C.F., Sanches Fernandes, L.F., Moura, J.P., Pacheco, F.A.L., 2019. Diagnosis of degraded pastures using an improved NDVI-based remote sensing approach: An application to the Environmental Protection Area of Uberaba River Basin (Minas Gerais, Brazil). Remote Sens. Appl. Soc. Environ. 14, 20–33. https://doi.org/10.1016/J.RSASE.2019.02.001

Van Ewijk, K.Y., Randin, C.F., Treitz, P.M., Scott, N.A., 2014. Predicting fine-scale tree species abundance patterns using biotic variables derived from LiDAR and high spatial resolution imagery. Remote Sens. Environ. 150, 120–131. https://doi.org/10.1016/j.rse.2014.04.026

Villamuelas, M., Fernández, N., Albanell, E., Gálvez-Cerón, A., Bartolomé, J., Mentaberre, G., López-Olvera, J.R., Fernández-Aguilar, X., Colom-Cadena, A., López-Martín, J.M., Pérez-Barbería, J., Garel, M., Marco, I., Serrano, E., 2016. The Enhanced Vegetation Index (EVI) as a proxy for diet quality and composition in a mountain ungulate. Ecol. Indic. 61, 658–666. https://doi.org/10.1016/j.ecolind.2015.10.017

Vogt, T., Gerhard Gul, P., 1994. Accumulation of flavonoids during leaf development in Cistus laurifolius. Phytochemistry 36, 591–597. https://doi.org/10.1016/S0031-9422(00)89780-0

Wachendorf, M., Fricke, T., Möckel, T., 2017. Remote sensing as a tool to assess botanical composition, structure, quantity and quality of temperate grasslands. Grass Forage Sci. 73, 1–14. https://doi.org/10.1111/gfs.12312

Weisberg, P.J., Coughenour, M.B., 2006. Modelling of large herbivore – vegetation interactions in a landscape context.

Westoby, M.J., Brasington, J., Glasser, N.F., Hambrey, M.J., Reynolds, J.M., 2012. "Structure-from-Motion" photogrammetry: A low-cost, effective tool for geoscience applications. Geomorphology 179, 300–314. https://doi.org/10.1016/j.geomorph.2012.08.021

Youngentob, K.N., Renzullo, L.J., Held, A.A., Jia, X., Lindenmayer, D.B., Foley, W.J., 2012. Using imaging spectroscopy to estimate integrated measures of foliage nutritional quality. Methods Ecol. Evol. 3, 416–426. https://doi.org/10.1111/j.2041-210X.2011.00149.x

Zhang, L., Huettmann, F., Liu, S., Sun, P., Yu, Z., Zhang, X., Mi, C., 2019. Classification and regression with random forests as a standard method for presence-only data SDMs: A future conservation example using China tree species. Ecol. Inform. 52, 46–56. https://doi.org/10.1016/j.ecoinf.2019.05.003

799 **TABLES**

800 **Table1.** Species and number of individuals (n) sampled in NGRPTB Iberian ibex enclosure. Species
801 are grouped by families and given a code to simplify the interpretation of the consequent analysis. Plant
802 life-forms agree with Raunkier´s classification (1934).

803

Family	Specie	CODE	n	Physiognomy
Anacardiaceae	*Pistacia lentiscus*	PL	20	Evergreen microphanerophyte with compound broad-leaves
Buxaceae	*Buxus sempervirens*	BS	6	Evergreen microphanerophyte with simple broad-leaves
Cistaceae	*Cistus albidus*	CA	8	Evergreen nanophanerophyte with simple broad-leaves covered by dense white tomentous
	Helianthemum marifolium	H	8	Evergreen loosely branched chamaephyte with tiny (< 10x10 mm) simple and hairy broad-leaves
Cupressaceae	*Juniperus oxycedrus*	JO	20	Evergreen microphanerophyte with simple needle-leaves.
Ericaceae	*Erica multiflora*	EM	20	Evergreen nanophanerophyte with tiny (< 10 mm length) simple linear-leaves
Fagaceae	*Quercus coccifera*	QC	20	Evergreen microphanerophyte with simple broad-leaves
	Quercus ilex	QI	20	Evergreen mesophanerophyte with simple broad-leaves
Labiatae	*Rosmarinus officinalis*	RO	20	Evergreen nanophanerophyte with simple linear-leaves
	Thymus vulgaris	TV	20	Evergreen chamaephyte with tiny (< 5 mm length) simple linear-leaves
Leguminosae	*Genista scorpius*	GS	8	Evergreen thorny and promptly leafless nanophanerophyte
	Ulex parviflorus	UP	11	
Oleaceae	*Phillyrea angustifolia*	PA	7	Evergreen microphanerophyte with simple lanceolate broad-leaves
Pinaceae	*Pinus nigra*	PN	10	Evergreen mesophanerophyte with simple needle-leaves
	Pinus pinaster	PP	10	
Palmae	*Chamaerops humilis*	CH	8	Evergreen nanophanerophyte with compound fan-like leaves
Graminoids	*Brachypodium phoenicoides*	BP	10	Evergreen tussock-like hemicryptophyte
	Brachypodium retusum	BR	10	
	Graminoids	G	10	

804

Table2. Image processing information for each flight executed in NGRPTB Iberian Ibex enclosure. The table includes season, flight height, surface recorded by the image, number of ground control points (GCP), calibration error (mean RMS error), number of recorded images and number of images used to create the model.

Month	Flight (m)	Surface (ha)	GCP	Mean RMS error (m)	No. Images	No. Calibrated images
June	30	2.8457	18	0.04-0.28	1013	868
June	60	5.8915	16	0.23-0.08	245	245
March	30	5.1267	21	0.03-0.07	2188	2152

824 **Table 3**. Plant species classification results obtained with a set of random forest models using digital
825 values of the three bands recorded by a BG-NIR camera (NIR, Blue and Green). Data collected using
826 a sUAS flying in July (2018) and March (2019) in the Iberian Ibex (*Capra pyrenaica*) enclosure in the
827 NGRPTB. Images were recorded at two heights (30 and 60 m) and different resolutions (3.5, 5, 10 and
828 30 cm pixel size). OOB error is the classification error according to the random forest algorithm. Test
829 error is the error obtained when comparing algorithm prediction results with test data not included in the
830 model development. We performed two kinds of classification:for the most abundant plants in the
831 enclosure (n = 19, All species), and for plants preferred by Ibexes (Diet). In the Diet group, plants have
832 been grouped in 4 types namely: *Cistus albidus*, *Erica multiflora*, Fagaceae (*Quercus coccifera* and *Q.*
833 *ilex*) and Graminoids (e.g., *Brachypodium phoenicoides, B. retusum* and other graminoids).

834

Response variables	Flight	Month	Resolution (cm)	OBB error (%)	Test error (%)
All species	low	March	30	70.89	70.66
	high	June	30	66.49	70.28
	low	March	10	69.14	68.56
	low	June	10	55.50	56.07
	low	June	5	53.24	52.73
	low	March	5	50.89	50.43
	high	June	10	50.03	49.19
	low	March	3.5	48.38	48.57
	high	June	5	43.54	43.77
	low	June	3.5	35.39	35.64
	low	June	30	68.99	29.78
	high	June	3.5	28.77	25.26
Diet	low	March	3.5	27.94	28.26
	low	June	3.5	23.51	23.87
	high	June	3.5	18.38	18.70

835

836

837

838

839

840

841

842

843

844

FIGURE CAPTIONS

Figure 1. The study area is placed in the National Game Reserve ‘‘Ports de Tortosa i Beseit’’ (NGRPTB) in Catalonia, northeast Spain (40º46’08’’ N, 0º20’04’’ E, 450 m. a. s. l.) marked in the upper inset. The yellow line marks the Iberian Ibex enclosure. The white area indicates the flight area.

Figure 2. Field sampling in the Iberian Ibex enclosure in NGRPTB. Up to 20 individuals of the most representative species of the area were marked with a dGPS. Insets present the species most consumed by Iberian ibex in the enclosure.

Figure 3. A) Monthly variation of mean NDVI values recorded in the Iberian Ibex enclosure, in the NGRPTB. Mean NDVI values corresponding to the 2014-18 period. Clear seasonal pattern evident with peak primary production in winter and minimum in summer. The asterisk indicates statistically significant differences between March and June NDVI (red bars). B) Variation of mean Blue-NDVI in the plants recorded in the Ibex enclosure in March and June calculated from the images obtained by a BG-NIR camera. All species have statistical differences (t-test) except for those marked with asterisks. *Brachypodium retusum* (BR), *Helianthemum marifolium* (H), and *Pinus pinaster* (PP). All plant species abbreviations are depicted in Table 2.

Figure 4. Diet composition assessed by a faecal micro-histological analysis of 10 faecal samples collected in the Ibex enclosure in December 2019. Bars represent the mean of the proportion of each plant species in our faecal samples. ONLW (Other Non-Legume Wood species), EM (*Erica multiflora*), G (*Brachypodium phoenicoides, B. retusum* and other graminoids), ONLF (Other Non-Legume Forb species), L-A (Labiatae-Asteraceae), QI (*Quercus ilex*), CA (*Cistus albidus*), TV (*Thymus vulgaris*), PL (*Pistacia lentiscus)*, HH (*Hedera helix*), CM (*Crataegus monogyna*), RU (*Rubus ulmifolius*), RO (*Rosmarinus officinalis*), GS (*Genista scorpius*), Sasp (*Smilax aspera*), L (Laminaceae), Dsp (*Dorycnium* sp.), A (Asteraceae), BS (*Buxus sempervirens*), I-O (Iridaceae-Orchidaceae), PA (*Phillyrea angustifolia*), Psp (*Pinus* sp.), Csp (*Carex* sp), Ssp (*Satureja* sp.), Rsp (*Rosa* sp.).

Figure 5. Mean scores from the first PCA dimension performed with NIR, Green and Blue band recordings on 19 plant species sampled in the NGRPTB vegetation study. All plant species abbreviations are depicted in Table 2.

Figure 6. Mean scores from the first PCA dimension performed with NIR, Green and Blue band recordings on 5 plant categories consumed by Iberian ibexes in the NGRPTB. ‘C’: *Cistus albidus*; ‘G’: *Brachypodium phoenicoides, B. retusum,* and other grass-like plants as Graminoids. ‘L’: *Rosmarinus officinalis* and *Thymus vulgaris* as the family Labiatae; ‘E’: *Erica multiflora;* ‘F’: *Quercus* spp. as the family Fagaceae.

Figure 7. Foodscape map overlayed with the infrared false-colour orthomosaic of the study area. Predicted categories are based on RFMl with an OOB error of 18.4%. A pie chart illustrates the proportion of the 6 dietary categories: ‘F’: *Quercus* spp. as the family Fagaceae; ‘L’: *Rosmarinus officinalis* and *Thymus vulgaris* as the family Labiatae; ‘E’: *Erica multiflora;* ‘C’: *Cistus albidus*; ‘G’: *Brachypodium phoenicoides, B. retusum,* and other grass-like plants as Graminoids. ‘Others’ category includes plants without dietary interest, bare soil and rock.

884

885 **FIGURES**

886

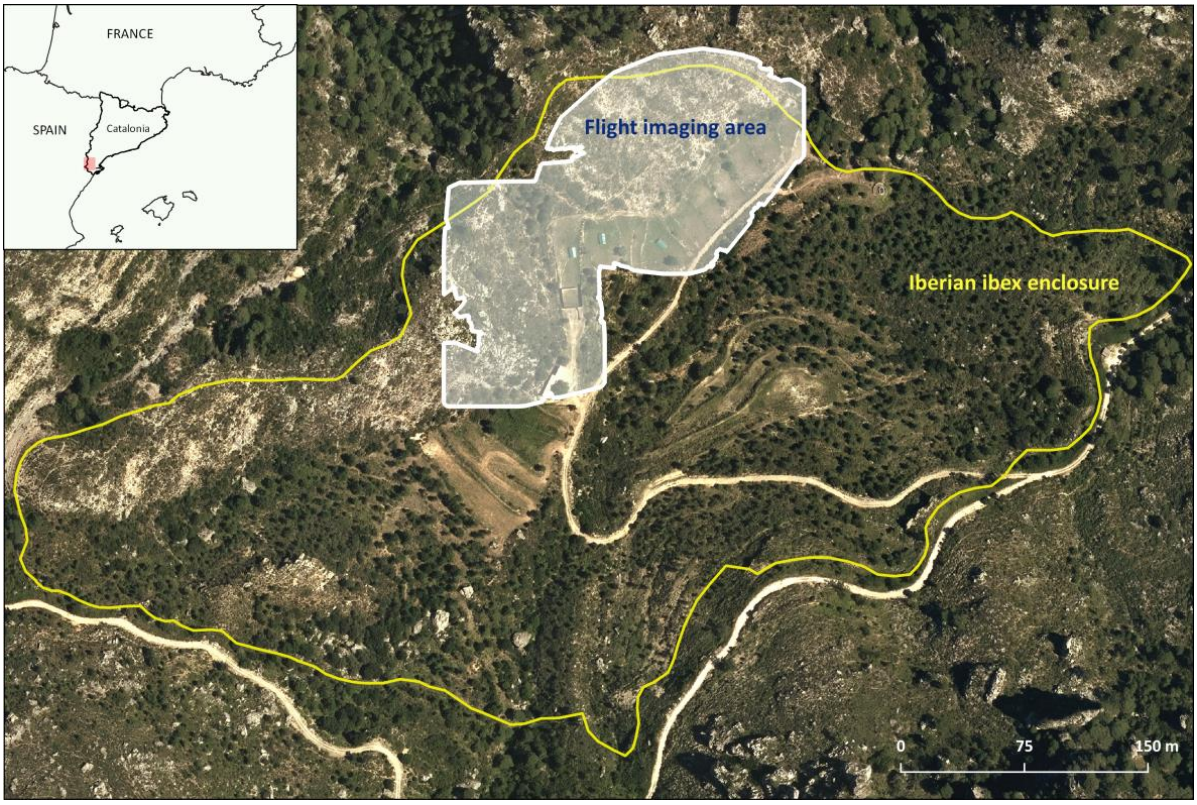

887

888 **FIGURE 1**

889

890

891

892 **FIGURE 2**

893

894

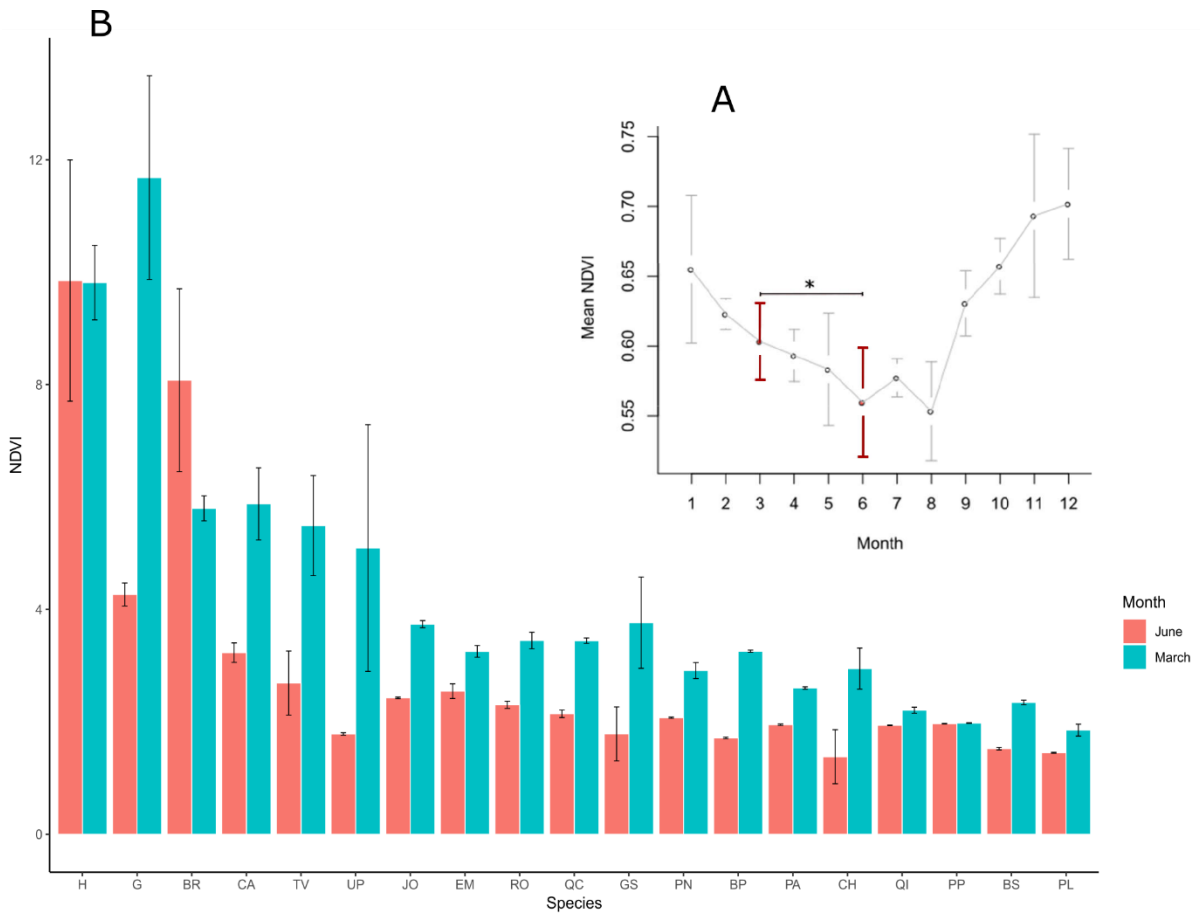
B
A
NDVI
Mean NDVI
Month
Species
Month
June
March
H
G
BR
CA
TV
UP
JO
EM
RO
QC
GS
PN
BP
PA
CH
QI
PP
BS
PL

FIGURE 3

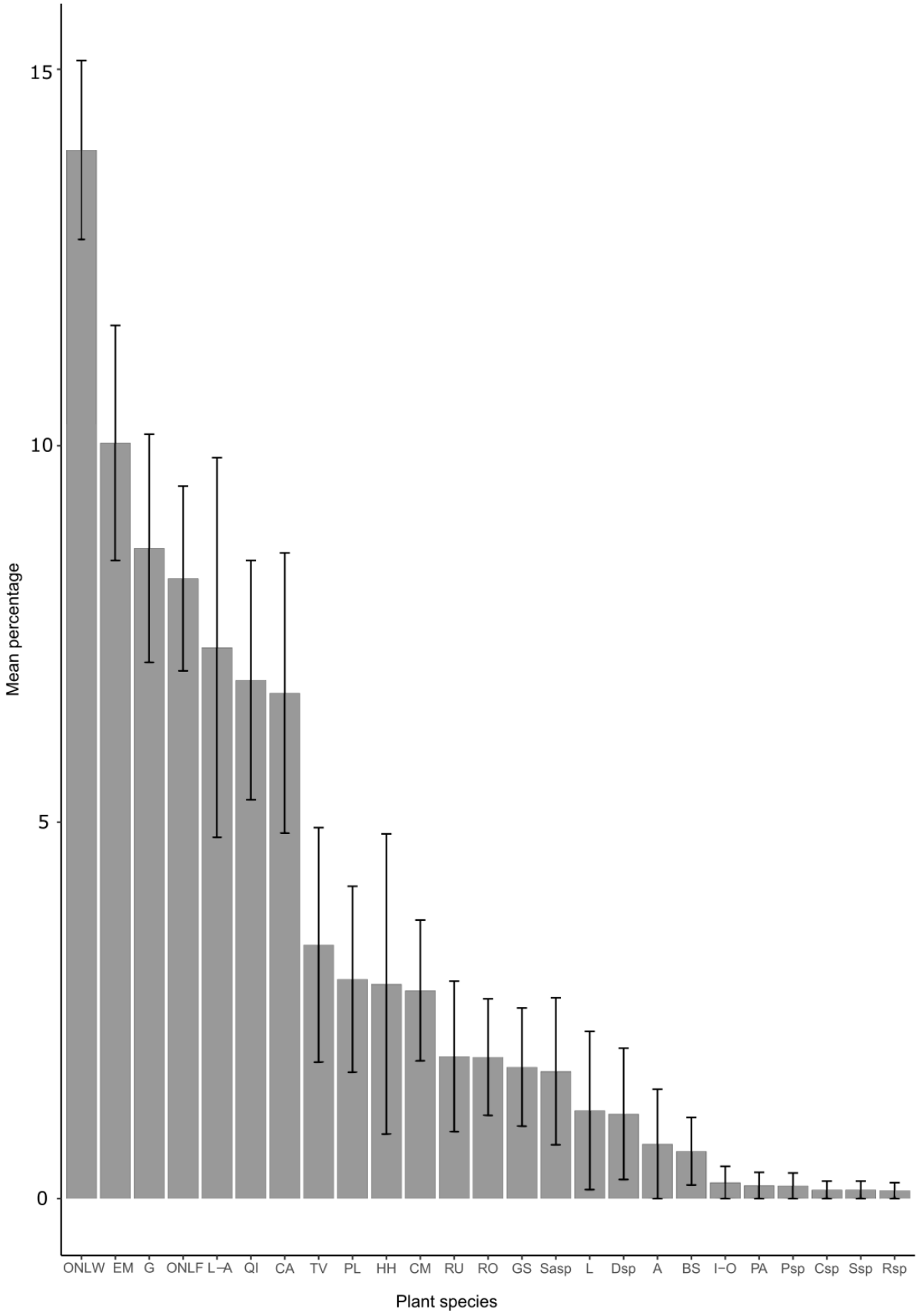
15
10
5
0
Mean percentage
ONLW EM G ONLF L–A QI CA TV PL HH CM RU RO GS Sasp L Dsp A BS I–O PA Psp Csp Ssp Rsp
Plant species

FIGURE 4

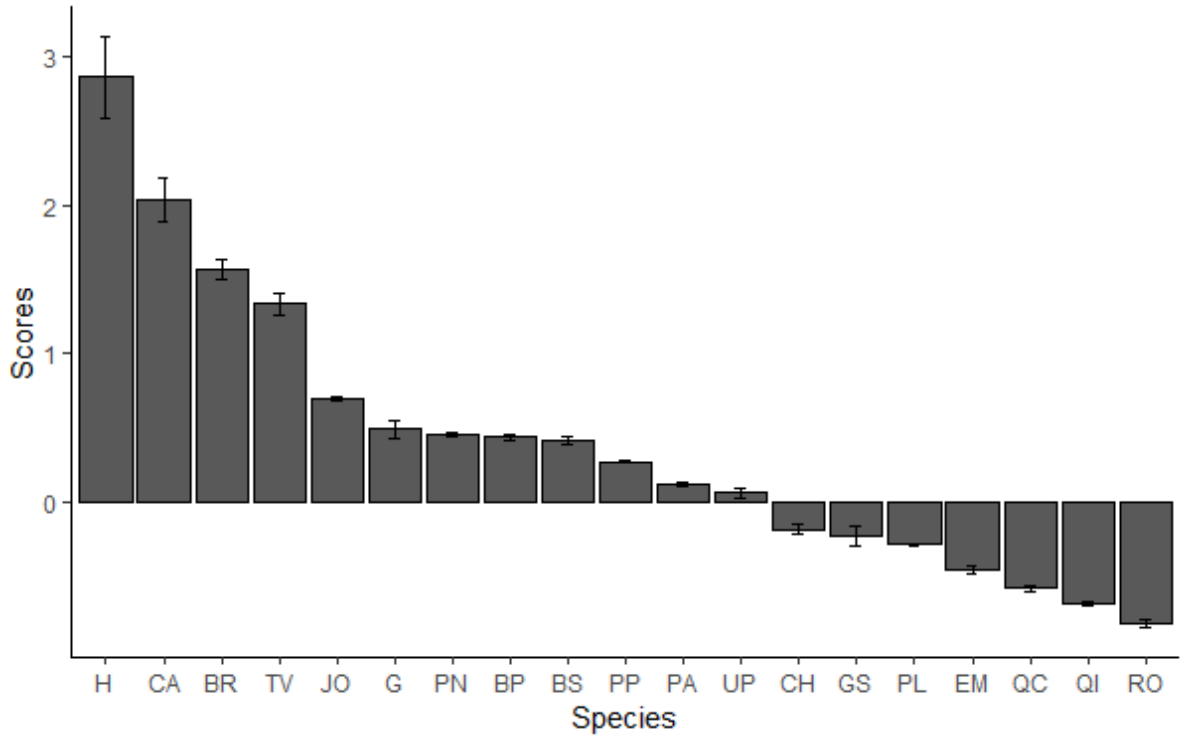
Scores
3
2
1
0
H
CA
BR
TV
JO
G
PN
BP
BS
PP
PA
UP
CH
GS
PL
EM
QC
QI
RO
Species

FIGURE 5

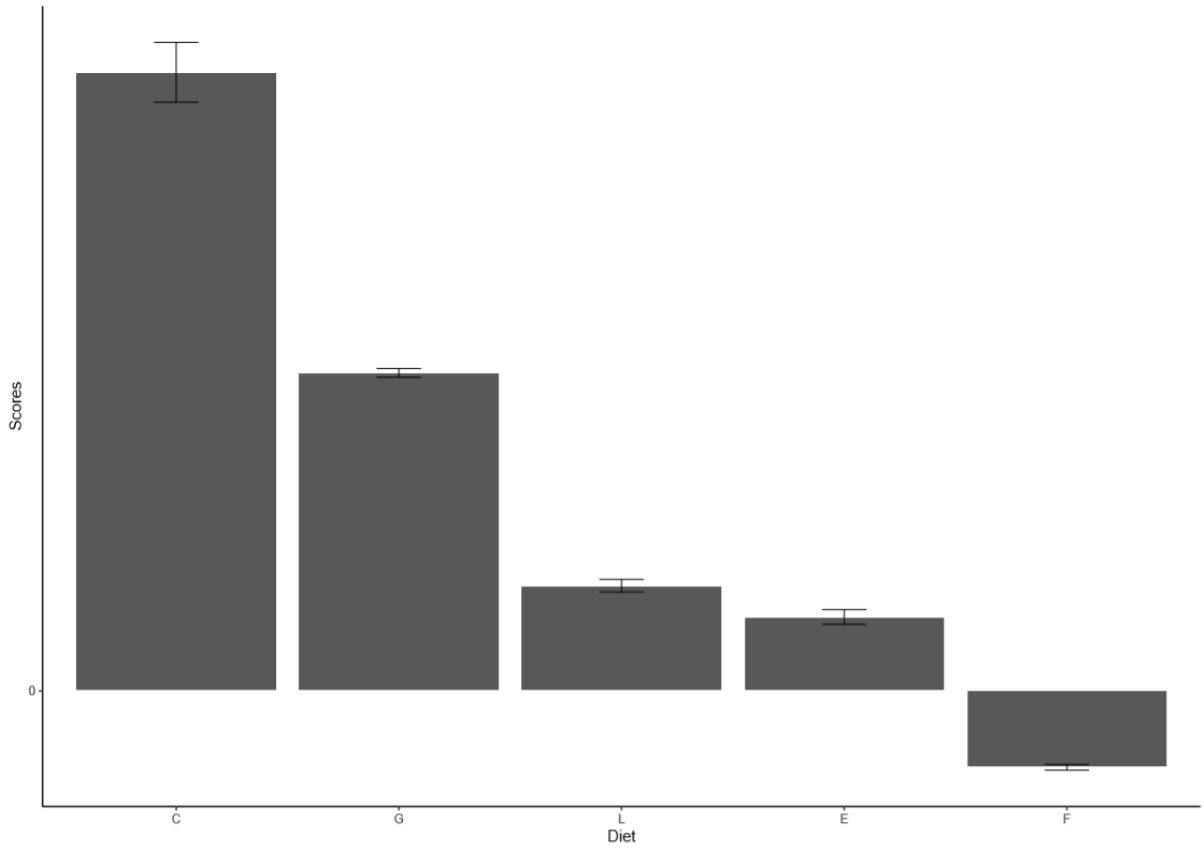

FIGURE 6

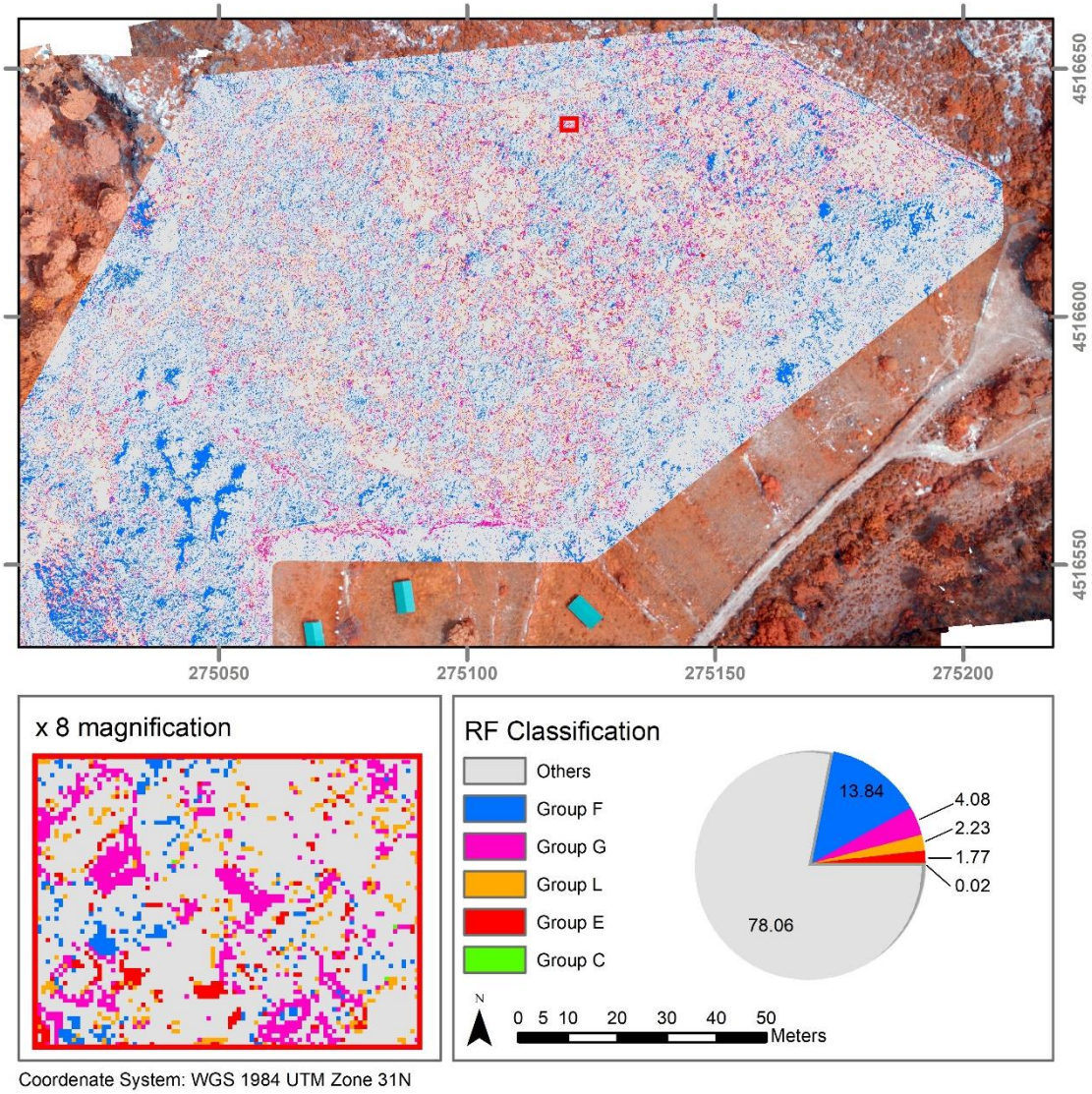
4516650
4516600
4516550
275050
275100
275150
275200
x 8 magnification
RF Classification
Others
Group F
Group G
Group L
Group E
Group C
13.84
4.08
2.23
1.77
0.02
78.06
N
0 5 10 20 30 40 50
Meters
Coordenate System: WGS 1984 UTM Zone 31N

FIGURE 7